# Effect of Interpolation on Electroanatomical Mapping

Margarita Sanromán-Junquera[1], Raquel Díaz-Valencia[1], Arcadio García-Alberola[2], José L Rojo-Álvarez[1], Inmaculada Mora-Jiménez[1]

[1] Universidad Rey Juan Carlos, Fuenlabrada (Madrid), Spain
[2] Hospital Virgen de la Arrixaca, Murcia, Spain

## Abstract

*Cardiac navigation systems (CNS) are often used in electrophysiological studies to create spatial-electrical maps supporting the arrhythmia mechanism identification. Sequentially recorded electrograms yield the bioelectrical information from features such as voltage and activation times in terms of their spatial location, which are subsequently interpolated for building the electroanatomical map (EAM) of the cardiac chamber. Our goal was to evaluate quantitatively the effect of interpolation in the EAM accuracy when reconstructed from a set of samples. Triangulated irregular networks (TIN), thin plate spline (TPS), and support vector machines (SVM) were assessed by using: (a) two detailed simulated time activation maps during flutter and sinus rhythm in both atria; (b) a set of real CNS maps, given by 13 activation time and 19 voltage maps, with 6 right atria (RA), 6 left atria (LA), 4 right ventricles (RV), and 16 left ventricles (LV). Interpolation methods were benchmarked using root mean squared error (RMSE), efficiency (EF), and Willmott distance (WD). On the one hand, EF and WD were similar for yielding a clearer cut-off point than RMSE for the number of required samples, which was about 100. Better EAM accuracy was obtained using TPS, followed by SVM and TIN, except for flutter in the RA, where early-meets-late was smoothed by SVM. On the other hand, EAM accuracy (in terms of the average WD) was slightly outperformed by RA than LA (0.57 vs 0.52), whereas RV and LV were similar (0.71 vs 0.71). In reference to the methods, similar average WD was given by the interpolation methods (TIN 0.64 $\pm$ 0.14; TPS 0.66 $\pm$ 0.15; SVM 0.65 $\pm$ 0.18). The EAM accuracy is dependent on the map nature and on the cardiac chamber.*

## 1. Introduction

Cardiac navigation systems (CNS) are usually used for cardiac mapping with the aim of identifying the arrhythmia mechanism and enhancing the ablation success during electrophysiological (EP) studies. These systems are capable of localizing and guiding catheters and electrodes within the heart by using electromagnetic fields. In addition, they build three dimensional electroanatomical maps (EAM), which show a cardiac feature, such as voltage amplitude or activation time, over an anatomical representation of the cardiac chamber surface in real time.

The newest CNS can create the anatomical mesh quickly by incorporating either anatomical information provided by a multi-electrode catheter, or medical images such as computed tomography and magnetic resonance. However, the electrical information is acquired by sequentially recording the electrical activity (electrograms or EGM) at multiple sites during several seconds. The higher the number of recorded EGM, the higher the accuracy of the EAM, although the EP study duration is also increased. Thus, the EAM is represented by an anatomical mesh, with a cardiac feature (such as voltage amplitude or activation time) measured and associated to several of the mesh vertices [1].

For an accurate representation of the EAM, the cardiac feature is interpolated in the rest of the vertices where the EGM were not recorded. Therefore, the aim of this work was to evaluate quantitatively the effect of the interpolation in the accuracy of the reconstructed EAM. For this purpose, triangulated irregular networks (TIN), thin plate spline (TPS), and support vector machines (SVM) were benchmarked for the cardiac feature interpolation in simulated and real EAM, and in both ventricles and atria.

This paper is structured as follows. In the next section, we summarize the assessed interpolation methods. In Section 3, we present the results of the interpolation for the cardiac features in simulated and real EAM. Conclusions are finally summarized.

## 2. Interpolation methods

In order to evaluate the accuracy of different EAM reconstructions, we considered three interpolation methods.

**TIN** method uses the Delaunay triangulation to build adjacent, continuous and non-overlapping triangles from irregularly spaced samples. The Delaunay triangulation is done such that the unique circle circumscribed about each triangle contains no other samples in its interior. This def-

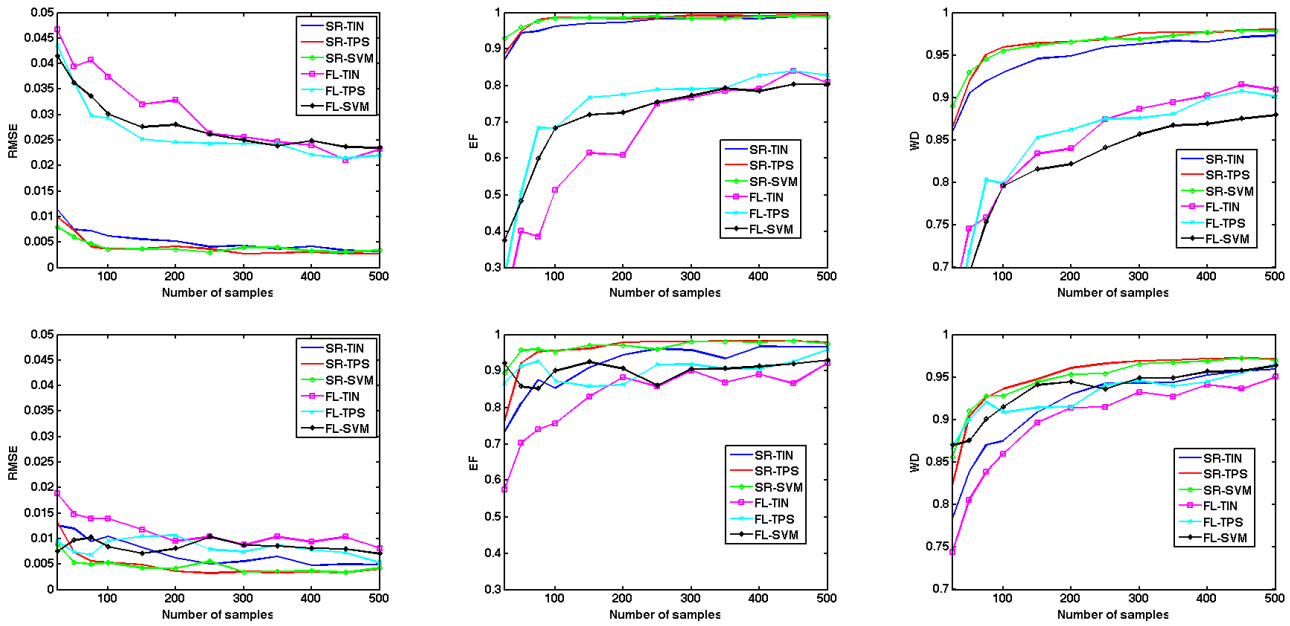


Figure 1. Evolution of RMSE, EF and WD with the number of samples and for a flutter (FL) and sinus rhythm (SR) simulation in the right atrium (superior) and left atrium (inferior) using TIN, TPS and SVM.

inition can be extended to higher dimensions. The principles of TIN are described in detail in [2].

**TPS** method estimates a thin smooth surface that passes through all given samples. This surface is constructed by selecting a function minimizing the bending energy of a surface [3]. Despite a TPS was initially motivated for a two dimensional interpolation scheme, the concepts can be applied to any dimension [4,5]. Unlike TIN, if noise is presented in the samples, a regularization parameter $\lambda$ allows to relax the interpolation requirements, and then, the resulting surface does not cross exactly through the samples.

**SVM** is a learning algorithm based on the Structural Risk Minimization principle [6]. This method maps the samples (as input vectors) to a high-dimensional space through a nonlinear mapping, so that it is possible to estimate a regression hyperplane in this space. The nonlinear mapping is done by using a Mercer kernel, the most usual one being the Gaussian kernel. In the training process, the regularization parameter, $C$, the percentage of support vectors, $\nu$, and the Gaussian width, $\sigma$, are searched and tuned.

In order to design the TPS and SVM interpolators, we explored a range of values for each design parameter in every method:

- For parameter $\lambda$ in the TPS method, values were considered between $\lambda = 10^{-3}$ and $\lambda = 10^{2}$ in 10 logarithmically-spaced intervals.
- For percentage of support vectors ($\nu$), the range was evaluated from 0.1 to 0.95 in 10 equidistant intervals.
- For the Gaussian width, $\sigma$, the range from $0.1\hat{\sigma}$ to $2\hat{\sigma}$ was searched in 10 equidistant intervals, where $\hat{\sigma}$ is the mean distance between each pair of samples, where the term *samples* refers to vertices with a cardiac feature (EGM) associated.
- For parameter $C$, values between $C = 10^{0}$ and $C = 10^{2}$ in 4 logarithmically-spaced intervals were considered.

While the most appropriate parameter value for TPS was chosen according to a *leave-one-out* (LOO) methodology, a 5-fold cross-validation approach was used for SVM due to the high computational time required to search three different parameters with the LOO methodology [7].

## 3. Results

The interpolation methods were assessed by using the LOO strategy, and several merit figures were used for this evaluation: root mean squared (RMSE), efficiency (EF), and Willmott distance (WD) [8].

**Interpolation for simulated EAM**. Simulated activation time EAM for two rhythms, a sinus rhythm (SR) and a flutter (FL) in the right atrium [9, 10], were interpolated by using the three proposed methods, namely, TIN, TPS, and SVM. Given that simulated EAM have tens of thousands of vertices and the real CNS EAM have barely hundreds of vertices, simulated EAM meshes were irregularly and randomly subsampled with 25, 50, 75, 100, 150, 200, 250, 300, 350, 400, 450, and 500 vertices, in order to have a similar number of vertices as real EAM.

Figure 1 shows the average of RMSE, EF and WD with

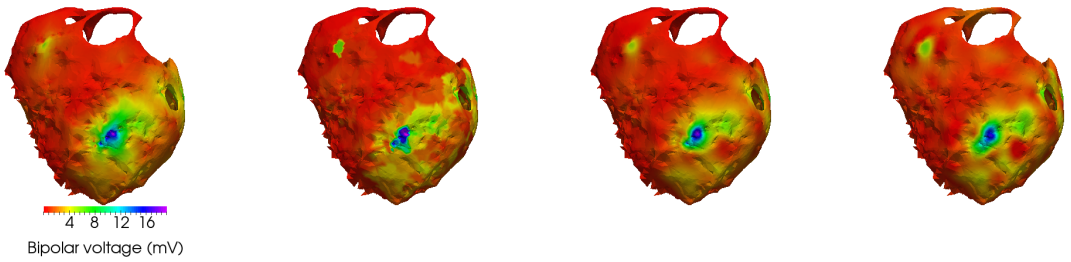


(a)

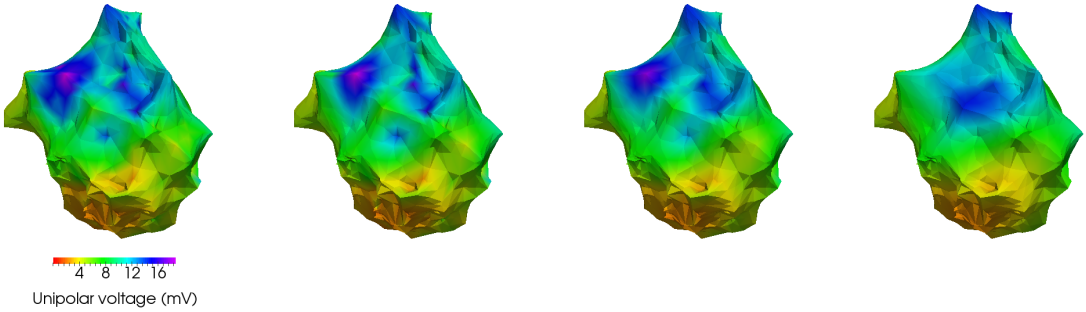


(b)

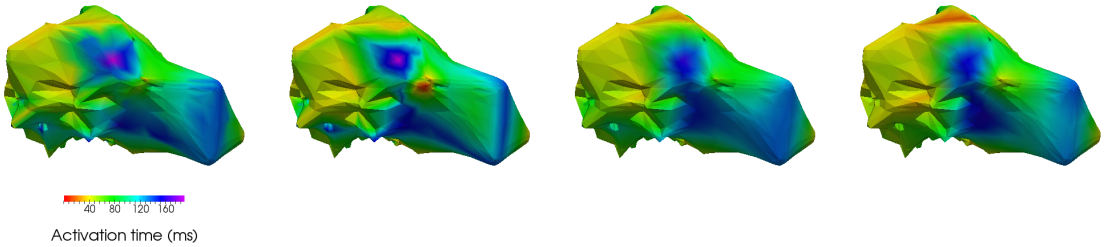


(c)

Figure 2. From left to right: Original EAM and the corresponding interpolation maps using TIN, TPS, and SVM for bipolar voltage (a), unipolar voltage (b), and activation time (c), in left ventricles.

Table 1. Average of RMSE, EF and WD, for bipolar and unipolar voltage (mV) and activation time (ms) in real CNS EAM, for the RA, LA, RV and LV using TIN, TPS and SVM.

| Cardiac chamber | Cardiac feature | No. EAM | TIN | | | TPS | | | SVM | | |
|---|---|---|---|---|---|---|---|---|---|---|---|
| | | | RMSE | EF | WD | RMSE | EF | WD | RMSE | EF | WD |
| RA | Bipolar | 2 | 0.67 | 0.03 | 0.53 | 0.61 | 0.23 | 0.68 | 0.61 | 0.21 | 0.62 |
| | Unipolar | 0 | - | - | - | - | - | - | - | - | - |
| | Activation | 4 | 81.00 | 0.03 | 0.56 | 67.74 | 0.33 | 0.72 | 65.95 | 0.38 | 0.71 |
| LA | Bipolar | 1 | 1.07 | 0.10 | 0.55 | 0.872 | 0.4 | 0.77 | 0.95 | 0.28 | 0.68 |
| | Unipolar | 0 | - | - | - | - | - | - | - | - | - |
| | Activation | 5 | 85.04 | -0.60 | 0.52 | 67.19 | 0.052 | 0.52 | 63.39 | 0.19 | 0.48 |
| RV | Bipolar | 1 | 1.76 | 0.26 | 0.61 | 1.57 | 0.41 | 0.80 | 1.57 | 0.41 | 0.80 |
| | Unipolar | 2 | 1.92 | 0.77 | 0.83 | 2.74 | 0.73 | 0.92 | 2.51 | 0.78 | 0.93 |
| | Activation | 1 | 26.27 | -0.07 | 0.56 | 27.22 | 0.34 | 0.74 | 24.73 | 0.44 | 0.77 |
| LV | Bipolar | 8 | 1.56 | 0.41 | 0.69 | 1.5 | 0.46 | 0.80 | 1.28 | 0.57 | 0.81 |
| | Unipolar | 5 | 1.95 | 0.72 | 0.78 | 1.73 | 0.78 | 0.93 | 1.87 | 0.73 | 0.92 |
| | Activation | 3 | 55.07 | -0.33 | 0.48 | 44.47 | 0.13 | 0.61 | 47.34 | 0.05 | 0.27 |

10 realizations for the simulated SR and FL in a RA and a LA. Lower performance was obtained in all methods and merit figures for FL in RA due to the high variation of the cardiac feature in the *early-meets-late* area of the activation EAM in a FL. EF and WD were similar for yielding a clearer cut-off point than RMSE for the number of required samples, which was around 100 atrial samples. In general, higher performance was obtained for TPS and SVM than for TIN; however TPS, and TIN yielded better EAM quality than SVM in FL-RA for the highest number of samples (from 400 to 500 in RMSE and EF, and from 150 to 500 in WD) due to the high smoothing in the *early-meets-late* created by SVM.

**Interpolation for real EAM**. Real CNS maps (13 activation time and 17 voltage maps) in 6 right atria (RA), 6 left atria (LA), 4 right ventricles (RV), and 16 left ventricles (LV), were also used to evaluate the performance of the interpolation methods (TIN, TPS and SVM). The CNS EAM had an average of $204 \pm 211$ samples ($105 \pm 40$ for RA, $123 \pm 44$ for LA, $164 \pm 175$ for RV, and $287 \pm 270$ for LV).

Table 1 shows the average for RMSE, EF, and WD in bipolar and unipolar voltage, and activation time EAM, for each interpolation method. TPS and SVM yielded better performance than TIN for almost all the EAM and cardiac chambers. Higher EF was yielded for unipolar voltage EAM than for bipolar, and activation time for both LV and RV. While the best bipolar voltage EAM quality was obtained with RA, the best activation time EAM quality was yielded in the RV.

Figure 2 shows the original and the corresponding interpolation maps with TIN, TPS and SVM for a bipolar voltage (a), unipolar voltage (b), and activation time (c) EAM. Given that there is no gold-standard for comparison, we used the EAM created by the CNS as reference. In the unipolar EAM, while the SVM method smooths the region of highest voltage, TPS and TIN are more similar to the interpolation generated by a real CNS. In the activation time EAM, both TPS and SVM smooths the region of latter activation, and TIN enhances the region of early activation.

## 4. Conclusions

CNS EAM are built by acquiring the anatomical shape of the cardiac chamber and creating a mesh where the electrical information, i.e. the cardiac feature, is added in several vertices where the EGM is recorded. In the rest of the vertices, the cardiac feature is interpolated in order to have a complete representation of the EAM. The accuracy of this interpolation determines the quality of the EAM, and hence, the clinical meaning to determine the arrhythmia mechanism and the best ablation treatment. Here, we evaluated three different interpolation methods, TIN, TPS and SVM, in simulated and real CNS EAM. In general, TPS and SVM yielded better performance than TIN, but the EAM accuracy is dependent on the map type and on the cardiac chamber.

## Acknowledgements

This work was partly supported the Spanish Government with Research Projects TEC2013-48439-C4-1-R and TEC2010-19263 from Ministerio de Economía y Competitividad. Special thanks to Dr. J Saiz and Dr. B Trenor in Universidad Politécnica de Valencia for providing the simulations.

## References

[1] Damiano RJ, Mark-Estes-II N, Marchlinski F. Interventional Cardiac Electrophysiology: A Multidisciplinary Approach. Cardiotext Publishing, 2015.

[2] Burrough P. Principles of geographical information systems for land resources assessment. Oxford, Clarendon Press, 1986.

[3] Duchon J. Splines minimizing rotation-invariant seminorms in sobolev spaces 1990;57:85–100.

[4] Meinguet J. Multivariate interpolation at arbitrary points made simple. Journal of Applied Mathematics and Physics ZAMP 1979;30:292–304.

[5] Wahba G. Spline models for observational data. CBMS-NSF Regional Conference Series in Applied Mathematics, Society for Industrial and Applied Mathematics (SIAM), 1990.

[6] Vapnik V. The Nature of Statistical Learning Theory. Springer-Verlag, New York, 1995.

[7] Bishop CM. Pattern Recognition and Machine Learning (Information Science and Statistics). Springer-Verlag New York, Inc., 2006.

[8] Willmott C, Robeson S, Matsuura K. Short communication - a refined index of model performance. International Journal of Climatology 2012;32:2088–2094.

[9] Tobón C, Ruiz-Villa C, Heidenreich E, Romero L, Hornero F, Saiz J. A three-dimensional human atrial model with fiber orientation. electrograms and arrhythmic activation patterns relationship. PLOS ONE 2013;8(2):e50883.

[10] Dux-Santoy L, Sebastian R, Felix-Rodriguez J, Ferrero J, Saiz J. Interaction of specialized cardiac conduction system with antiarrhythmic drugs: a simulation study. IEEE Transactions on Biomedical Engineering 2011;58(12):3475–8.

Address for correspondence:

Margarita Sanromán-Junquera
D-207, Departamental III, Universidad Rey Juan Carlos
Camino del Molino s/n, 28943-Fuenlabrada, Madrid (Spain)
E-mail to margarita.sanroman@urjc.es